

# Multimedia Application to the Simulation of Human Musculoskeletal System: A Visual Lower Limb Model from Multimodal Captured Data

Nadia Magnenat-Thalmann, Caecilia Charbonnier, Jérôme Schmid

*MIRALab, University of Geneva*

thalmann, charbonnier, schmid@miralab.unige.ch

**Abstract**—Musculoskeletal disorders are the most notorious and common causes of severe long-term pain and physical disability, affecting hundreds of millions of people across the world. To prevent and treat these disabling conditions, we are building an accurate generic lower limb model (consisting of bones and soft tissues) that can be simulated in motion, using individual multimodal data. For clinical every-day use, medically relevant validation and an efficient interactive visualization framework are required. Relevant patient’s anatomical, kinematical and mechanical data extracted from images (MRI), motion capture (dynamic MRI, optical motion capture) and other modalities (body scanning, EMG, mechanical properties measuring device), as well as statistical data, are adjusting the generic model to the patient. A fully functional model will be presented with some individual case studies and medical validation.

## I. INTRODUCTION

Since more than two decades, research in medical imaging has been continuously developed. Many aspects have been addressed as segmentation, topological modeling, simulation of physical processes, analysis of movements and validation of models [1], [2], [3], [4]. These efforts were primarily directed toward the display and visualization of extracted data from Computed Tomography (CT) or Magnetic Resonance Imaging (MRI). Nowadays, clinicians can obtain a complete 3D view of the volume of a human organ. One of the first generic model that demonstrated the complete pipeline from the acquisition of images to the construction of the topological model and its physics based simulation was done inside the European Project CHARM [5]. In this project, we worked on the simulation of the shoulder. We used CT data coming from the visible data set (Fig. 1) and we interpreted and labeled these images [6]. Then, we used a contour based technique to allow a control of the shape and the resolution of the geometry. We also developed a topological modeler that played the role of a 3D connectivity graph of anatomical elements for the shoulder [7]. In order to simulate the motion of the shoulder, finite element methods and kinematic joint motions were used [8]. This kind of approach needs a lot of research and attention, and is heavily going on. This 3D functional modeling research is a truly multidisciplinary approach that requires knowledge in system theory, mechanical engineering, mechanical design, human-machine interface, optimization, medicine, anatomy, orthopaedics and radiology.

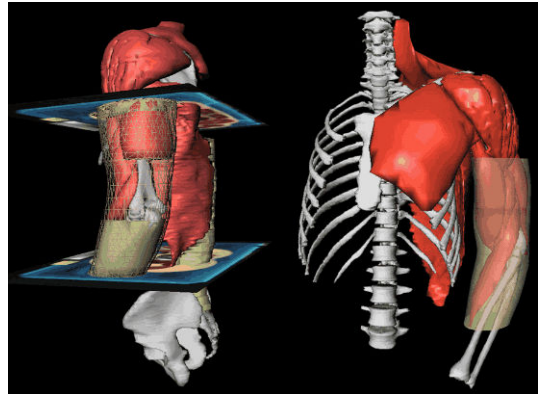


Fig. 1. **Shoulder Musculature Modeling**: One of the first attempts to model musculoskeletal structures (CHARM project [5]).

The musculoskeletal system is very complex and large anatomical variations exist among individuals. As a result, no modeling method has proven to be generic, automatic and robust. In many cases, anatomical modeling is interactive and time consuming [9], [10], [11], or not individualized [12]. For deriving the motion of the skeleton, various methods with direct access to the bone (e.g., intra-cortical pins [13], external fixators [14], percutaneous trackers [15]) have been proposed. These techniques are robust, but are strongly invasive. Therefore, the optical motion capture system seems to be the non-invasive solution for studying the kinematics of the joint. However, due to soft tissue deformation, reflective markers are subject to large displacement during movement (e.g., 20 mm for a marker stuck on the thigh). The resulting estimation are thus embedded with artifact. To minimize this effect, mathematical approaches have been implemented [16], [17], [18], but these techniques are limited to the use of non subject-specific models or are based on invalid assumptions. In this paper, we would like to illustrate the progress that has been done recently in 3D functional modeling. As an example, we will discuss the research done in two research projects: the European project 3D Anatomical Human [19] and the Swiss National project Co-Me [20]. Both projects aim to work on the functional simulation of the hip joint from MRI data. The main innovation in the pipeline from segmentation toward 3D

simulation is that 1) we work from MRI data and not CT, which is less invasive and 2) the novelty of the algorithms allows the process to be almost automatic and most of the cases in real-time. In addition, we try to take advantage of our know-how in scan technology and motion capture in order to visualize a full human with outer skin and hip organs in a functional simulation. We also do not work anymore on a generic patient only, but on patient-specific case studies. It means that in the next future, we will be able to see in 3D each patient's articulations and further predict what will happen if a specific motion is performed.

## II. DATA ACQUISITION

### A. Static Acquisition

1) *Magnetic Resonance Imaging (MRI)*: In case of musculoskeletal modeling, the visualization of soft and bony tissues is fundamental. Despite a good visualization of bones, CT is not truly appropriate for soft tissue examination such as muscles and ligaments. Furthermore, CT is an invasive modality whereas it is admitted that MRI does not create any harmful ionizing radiation [21]. The diversity of factors accounted by the MRI signal (e.g., proton density, T1 and T2 relaxation times, fluid flow) grants to MRI a unique versatility. For instance, a fluid flow/ tissue relationship is exploited in Diffusion tensor MRI to extract the muscle fiber direction. This provides an essential biomechanical parameter [22].

MRI protocols depend on the medical context and are subjected to the ubiquitous image quality-speed trade-off. Since we want to fully cover the hip and the thigh, we devised a protocol [23] that adjusts the slice thickness (from 2 mm to 10 mm) according to the region of interest. Indeed, an accurate (isotropic) acquisition of the whole area cannot be carried out in a reasonable time from a clinical viewpoint. The result is eventually a combination of different overlapping datasets that are registered together (Fig. 2). The acquisitions are performed on a 1.5T Intera MRI system manufactured by Philips Medical Systems.

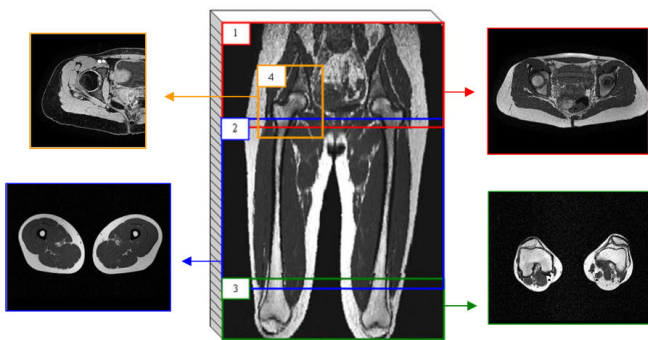


Fig. 2. **Static MRI protocol:** ● Axial 2D T1 Turbo Spin Echo (TSE), TR/TE= 578/18 ms, FOV/Matrix= 40 cm/512 × 512, thickness= 2 (hip (1)), 4 (knees (3)) or 10 mm (thigh (2)), gap/FA= 0 mm/90 deg, resolution= 0.78 × 0.78 mm. ● Axial 3D T1 Gradient-Echo (GE), TR/TE= 20/7 ms, FOV/Matrix= 20 cm/256 × 256, thickness= 2 mm (4), gap/FA= 0 mm/50 deg, NSA/resolution= 2/0.78 × 0.78 mm. Reproduced from [23]

2) *3D Body Scanning*: Body scanning is a modality that digitalizes accurate skin models of the complete body (accuracy  $\approx 1$  mm). The volunteer undergoes a 3D body scan (Vitus Pro, Vitronic, Germany) with the same markers set-up used for recording movements with the optical motion capture system. In this study, the use of body scan information is twofold. On the one hand, the 3D surface of the subject's body is generated and integrated in the visualization framework. On the other hand, the position of the markers on the skin can be extracted from the scan data, since the subject is captured with the markers. This information is further used in the optical motion capture process (more details in Section IV-B).

### B. Kinematical Acquisition

1) *Optical Motion Capture (MoCap)*: Optical motion capture provides a very practical and realistic way to animate virtual human bodies and to record joint kinematics. Such systems are not invasive and can be combined with force-plates and EMG for assessing musculoskeletal dynamics. Unlike other motion acquisition devices, the optical system allows the recording of a large range of motion. The markers trajectories are tracked within a 45.3 m<sup>3</sup> measurement volume (3.6 x 4.2 x 3 m) using 8 infrared cameras (Vicon MX 13i, Oxford Metrics, UK), sampling at 120 Hz. Two clusters of six 7 mm markers are affixed onto the lateral and frontal aspects of both thighs. Six markers are also stuck on the pelvis (Fig. 4A). Skin markers are arranged to ensure their visibility to the cameras throughout the range of motion. Additional reflective markers are distributed over the body to confer a more complete visualization from general to detailed. Data from the subjects are acquired from ordinary and sportive activities.

2) *Dynamic MRI (dMRI)*: Motion analysis can improve the diagnosis, especially the understanding of joint related pathologies (e.g., hip impingements). Dynamic MR imaging therefore appears as an appropriate modality to track the exact motion of musculoskeletal structures. But dMRI is significantly affected by technical and safety limitations (e.g., gradient strength, slew rate, signal-to-noise ratio). Fast acquisitions are thus performed at the expense of significant reductions in image quality and spatial coverage. Movements are also restricted by the MRI tube dimensions. Open MRI offers promising alternatives for the examination of a larger range of motion, but the magnetic field strength (<1 Tesla) limits the resolution. In order to avoid the shortcomings of large motion analysis in dMRI, we will exploit later on the capabilities of MoCap. Nevertheless, dMRI will be useful in validating the estimation of bone poses from MoCap data in case of low amplitude movements (more details in Section V). The chosen protocol for dMRI is a fast gradient echo sequence [24].

## III. GENERIC MODELS CONSTRUCTION

### A. Interactive Reconstruction

From a MRI dataset of a healthy patient, acquired with the proposed protocol, an interactive segmentation [23] is performed. A 2-simplex mesh [25], topologically equivalent to the structure to segment (e.g., a sphere or a cylinder),

is deformed to match the structure boundaries. The mesh is adapted according to a series of constraints defined as internal, external and boundary points. In an interactive manner, these points are placed by medical experts. To ensure the mesh quality an optimization process, based on geometrical and topological considerations, is applied. The result of this interactive segmentation is a collection of generic models of the various soft (cartilages, ligaments, muscles, skin) and bony structures. Various levels of details (LODs) for each mesh are then computed for a later exploitation in the individualized segmentation procedure.

### B. Joint Coordinate Systems

To report joint motion in a repeatable way that is independent from the acquisition frame, standard joint coordinate systems are computed from anatomical landmarks [26], [27], defined on the 3D reconstructed surface of the generic bones. These systems are implemented following the International Society of Biomechanics [27] (ankle and hip) and the seminal work of Grood and Suntay [26] (knee). They have been chosen to describe joint motion in clinically relevant terms (i.e., flexion/ extension, abduction/ adduction, internal/ external rotation).

### C. Topological Constraints

The human musculoskeletal system anatomy exhibits various organs interrelationships. For example, muscles are attached to bones, cartilages are fixed to specific bone areas, etc. This prior topological information can be taken into account to improve the segmentation or the computation of functional parameters (e.g., the hip joint center as described in Section IV-C). In soft tissue segmentation, topological constraints are therefore introduced for modeling bone/ soft tissue attachments. To this end, a method based on cardinal splines was developed to generate and parametrize attachment areas on the generic models. We defined about 50 generic attachment splines for the hip and the thigh, mainly from the literature on anatomy.

## IV. INDIVIDUALIZATION

### A. Segmentation

During the individualization phase, we apply a segmentation procedure that is equivalent to a Model to Image Registration. Generic models are firstly coarsely initialized before being deformed to match patient unique anatomy. The power of using and registering generic shapes is that exact geometric correspondences are obtained (i.e., morphological features have the same vertex indexes across individual models). A Thin-Plate Splines interpolation procedure initializes the generic bone models by using landmarks, placed at specific anatomical positions. On the other hand, soft tissues initialization exploits a skinning technique based on segmented bones. During the segmentation, models are considered as deformable meshes, driven by internal and external forces. Mesh vertices are thus modeled as particles with mass evolving under the Newtonian law of motion. This creates a Particle System

in which time-discretized differential equations relate particle states to forces. Time-integration is performed with a stable and robust integrator [28], [29]. The whole process uses a multi-resolution framework that accounts the different model LODs. A bottom-up forces propagation scheme [30] between the different resolutions linearly combines lower with higher resolution forces. This strategy brings robustness and speed to the segmentation procedure.

Internal forces regulate shape evolution by enforcing shape constraints. This is mainly done by using prior information that rely on assumptions about surface regularity (smoothness, curvature) and statistics on shapes variability. Based on a database of segmented models, a Principal Components Analysis expresses shape variations and rejects invalid shape configurations similarly to [31], [32]. Topological constraints are also exploited by individualizing the attachments. Spline control points are projected onto bone surfaces, while soft-tissues vertices are attached to the spline through curvilinear coordinates. Mass modification [33] is used to constrain these vertices. Finally, additional constraints are obtained by exploiting the medial axis representation of soft models like muscles [30].

External forces consider image information (e.g., intensity profiles and gradients) and non-penetration constraints. Intensity profiles [32], [25], [30] are intensity neighborhoods extracted along normals of models. Based on appropriate similarity measures, image forces are hence derived by registering generic intensity profiles with those of the evolving models. Collision handling [34] and response [35] techniques prevent models penetrations through speed/ position alterations or penalty forces.

### B. Skin Registration

From the 3D body scanner, a body contour of the subject is produced and accurately fitted to a generic body model [36]. This model needs to be replaced in the 3D space according to the position of the various organs, reconstructed from MR images. Moreover, the relative position of the skin markers is unknown with respect to the underlying bone. Since the subject was scanned with the skin markers, marker positions are extracted from the scan data using a least-squares sphere fitting technique. Subsequently, a registration method is used to conform the body model and the extracted marker positions to the generic skin segmented from MR images. Since the MRI skin model is limited to the pelvis and the femur, the registration method works in two phases (Fig. 3): 1) The body model surface from the pelvis to the knee is conformed to the MRI skin model through barycentric coordinates, previously stored from a single subject manual registration. 2) Rigid registrations are performed for the other body parts (i.e., the two shanks and the torso) using a least-squares minimization. Finally, markers which are attached to the body surface follow the transformation of the body model. As a result, the body model is replaced in the MRI space. A calibration frame is also obtained where the relative position of the skin markers, with respect to the underlying bone, is now established.

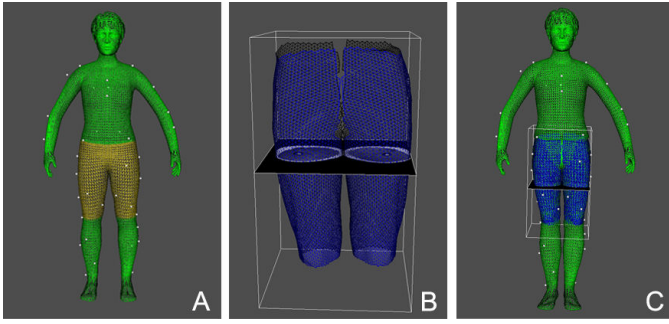


Fig. 3. A) The markers and the body model segmented into 2 parts: the yellow part is conformed to the MRI skin model and the green parts are rigidly registered B) The MRI skin model C) Registration result

### C. Motion Computation

In kinematic studies, the true hip joint center (HJC) is unknown since most techniques use external movement (motion capture data) or estimate its position relative to anatomical landmarks. With the present idea, the estimation of the HJC is first initialized with a geometrical approach: two topological areas (the femoral head and the acetabulum) are fitted with a sphere. Assuming a constant inter-articular distance, the best estimate of the HJC is given by centering the two spheres on the same point. Then, the algorithm adjusts the HJC by testing points around the initial guess, the goal being to minimize hip/femur bones collisions during low amplitude circumduction. The validation of this method can be found in [23].

When the human motion is measured using an optical motion capture system, the internal bone remains inaccessible and the resulting estimations are embedded with soft tissue artifacts (STA). Rigid motion of the bone segment can therefore not be robustly estimated from the markers trajectories, unless the STA is small. This “shifting” effect is very critical particularly when precise analyses of the joint motion are needed. To effectively reduce STA, we propose to use a global optimization that minimizes the error made globally for each instant frame on all the markers. Joint constraints are also applied so as to avoid non-physiological joint translation and dislocation.

During a movement, several components contribute to the motion of a skin marker. Assuming that the pelvis motion is known, the HJC can slightly move during the rotation of the thigh. This introduces one translation  $T_c$  and one rotation  $R$ . Additionally, a rigid displacement is observed due to STA which is denoted by another translation  $T_s$ . The motion of a marker with respect to the pelvis can hence be described by three transformations successively applied. Since an accurate estimation of both  $T_c$  and  $T_s$  is hardly possible, one of the translations must be discarded. Previous works [14], [37] showed that, for the thigh, the magnitude of the STA is greater than the displacement of the joint center. Therefore, we decide to compute the best estimate of  $T_s$  and to assume that  $T_c$  is close from null. Oppositely, for the pelvis, it appears that the STA remains small. Thus, for this bone we assume that  $T_s$  is close from null and we estimate  $T_c$  instead. Finally, the best transformation that minimizes the error made globally on the

markers is computed for each segment. The solution is given by minimizing the sum of squared distances between actual and model-determined marker positions. This is basically a least-squares minimization for which we use the rfsqp optimizer [38].

## V. VALIDATION AND RESULTS

To validate the automatic segmentation procedure, medical experts performed manual segmentations on four datasets. Following the generic construction approach, the required number of constraints points, necessary to reach satisfactory results, are placed. These “gold-standard” results were compared to those of the automatic segmentation. The mean distance (std. dev.) was 1.25 mm (1 mm) for bones and 1.7 mm (1.8 mm) for muscles. Since the expert editing remains prone to errors and the average distance is close to the image resolution ( $\approx 1$  mm), the proposed method is considered as accurate. Skin segmentation took around 60 sec and was visually validated. Moreover, the overall segmentation required around 15 min on a standard PC. This depicts a fast method given the complexity of the task. Cartilages and ligaments segmentation cannot be accurately identified in MRI (except maybe in arthro-MRI with contrast agent injection). Hence, a qualitative assessment was conducted. According to clinicians, a good agreement between 3D models and anatomical structures was found. Fig. 4B illustrates some of the results.

The validation of the joint kinematics estimation has been obtained using marker position data, collected during abduction motion patterns on 6 volunteers scanned with our dMRI protocol. The subjects were equipped with external MRI-compatible marker sets and a tracking device was used to ensure the movements repeatability. For each instant frame, the position and orientation of both the hip and femur bones were computed. The kinematics derived from the marker position data were compared with that of the MRI bone tracking. The root mean square reconstruction error was 2.3/3.9/4.1 mm in femur x/y/z translation and 2.3/1.4/1.9 deg in femur orientation. From these results, the errors in femur rotation are significantly reduced by applying the proposed method, with respect to the traditional ones. The translation errors are a bit more significant, but are strongly related to the magnitude of skin deformations during movements. Indeed, our validation data only featured markers on the thigh. Hence, we could only calculate the error made on the femur translation, which, as said previously exhibits a lot of skin motion and was thus discarded by our approach.

The proposed framework is applied to medical case studies. For example, relevant clinical output was obtained on a study involving professional ballet dancers. The motivation for this study was that dancers activities (extreme movements, repeated motion) can be at the origin of joint pathologies. Based on patient-specific reconstructed data, a support for standard morphological measurements [39], [40] was proposed, improving the (subjective) reading of medical images (Fig. 4D). Moreover, the visualization in real-time of patient-specific joints in extreme postures led the validation of clinical

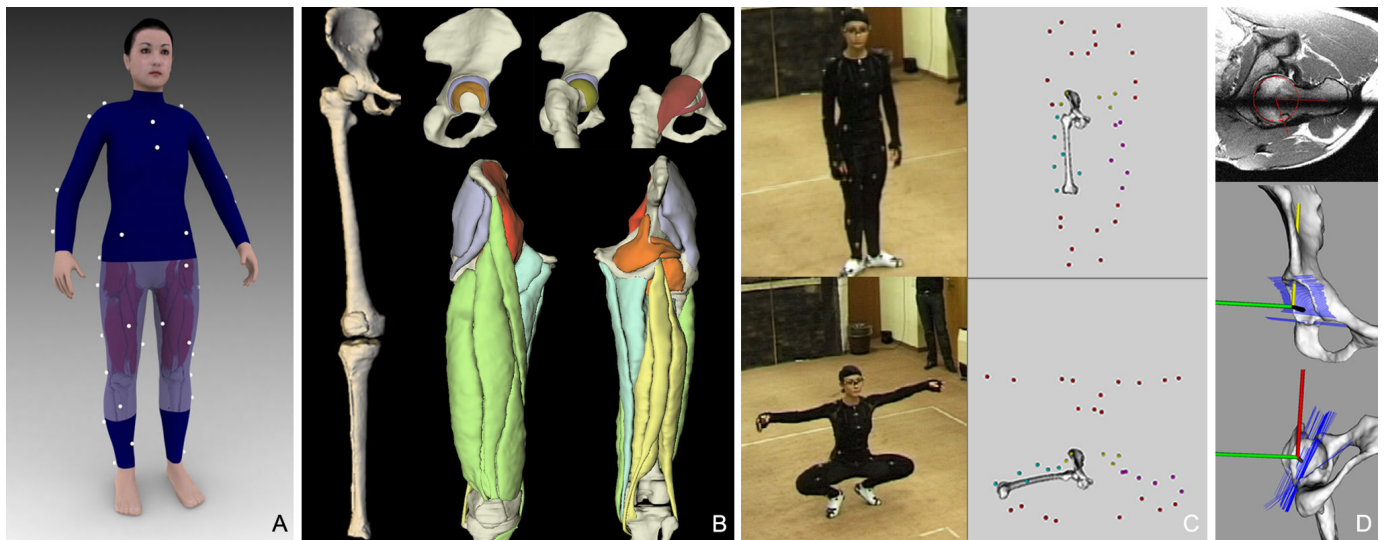


Fig. 4. A) Skin markers configuration B) Modeling results: bones (left), cartilages and ligaments (top) and muscles colored by anatomical groups (bottom) C) Real and computed postures from MoCap data (grand plié) D) Morphological measurements: alpha angle (top), acetabular version (middle and bottom)

assumptions. Indeed, unexpected bone/ cartilage collisions were observed during these extreme movements, establishing a correlation between the contact zone and diagnosed lesions. This confirms that motion can be a factor of joint degeneration. Fig. 4C shows examples of computed dancer's postures.

## VI. CONCLUSION AND FUTURE WORK

In the course of their work, clinicians are required to analyze large amounts of data related to musculoskeletal anatomy, kinematics, dynamics, mechanics and physiology. They must therefore manage and visualize information at increasing levels of complexity. To reduce this complexity and to exploit the information efficiently, it is fundamental to centralize and structure the multimodal data inputs in a comprehensive manner. In addition, the diagnosis is mainly based on static radiological images and external palpation that give information about the patients anatomy and joint mobility. However, in most of the pathological cases, it is also important to resort to biomechanics methodologies and motion protocols to analyze more precisely the pathology and to determine its causes. The proposed framework is specifically designed in this aim. The developed tools and the combined internal (bones and soft tissues)/ external (skin) functional visualization of the subject provides a more comprehensive view of the joint configuration and is expected to support the diagnosis.

Future work will address the following points that are scheduled in Co-Me [20] and 3D Anatomical Human [19] projects. Firstly, a more thorough validation of the multimodal modeling will be conducted. Segmentation accuracy will be improved, especially regarding cartilage extraction, as currently a quantitative validation is missing. Following, additional dMRI experiments will be carried out to estimate the error made on the pelvis translation. Secondly, additional acquisition devices such as EMG and force-plate will be added to the framework to provide valuable biomechanical parameters. Finally, the

complex mechanical behavior of musculoskeletal tissues (e.g., biphasic, viscoelastic, non linear, etc.) will be simulated to highlight abnormal stress distributions in case of pathological patients. This will demand effort in volumetric meshing, simulation and mechanical parameters measurement.

## ACKNOWLEDGMENT

This work is supported by the Co-Me project funded by Swiss National Research Foundation and by the 3D Anatomical Human project funded by the European Union. We would like to thank the University Hospital of Geneva, Professor Pierre Hoffmeyer, Lazhari Assassi, Pascal Volino, Marlène Arévalo and Nedjma Cadi for their collaboration. We are also grateful to all volunteers from the ballet of the Great Theater of Geneva to have accepted to take part in the study.

## REFERENCES

- [1] L. Brown, "A survey of image registration techniques," *ACM Comput Surv*, vol. 24, no. 4, pp. 325–376, 1992.
- [2] M. Bro-Nielsen and S. Cotin, "Real-time volumetric deformable models for surgery simulation using finite elements and condensation," *Comput Graph Forum*, vol. 25, no. 3, pp. 57–66, 1996.
- [3] S. Narayan, D. Sensharma, E. Santori, A. Lee, A. Sabherwal, and A. Toga, "Animated visualization of a high resolution color three dimensional digital computer model of the whole human head," in *Year book of Medical Informatics*, IMIA-Schattauer, Ed., 1994, pp. 482–501.
- [4] M. Kass, A. Witkin, and D. Terzopoulos, "Snake: Active contour models," *Int J Comput Vis*, vol. 1, no. 4, pp. 321–331, 1987.
- [5] (1993-96) Charm website, esprit project 9036. [Online]. Available: <http://ligwww.epfl.ch/maurel/CHARM/>
- [6] P. Gingins, P. Kalra, P. Beylot, N. Magnenat-Thalmann, and J. Fasel, "Using vhd to build a comprehensive human model," in *The Visible Human Project Conf Proc (CD-ROM)*, 1996.
- [7] P. Kalra, P. Beylot, P. Gingins, N. Magnenat-Thalmann, P. Volino, P. Hoffmeyer, J. Fasel, and F. Terrier, "Topological modeling of human anatomy using medical data," in *Comput Anim*, 1995, pp. 172–180.
- [8] W. Maurel, Y. Wu, N. Magnenat-Thalmann, and D. Thalmann, *Biomechanical Models for Soft Tissue Simulation*, ser. Basic Research. New York: Springer-Verlag, 1998.
- [9] J. Teran, E. Sifakis, S. Blemker, V. Ng-Thow-Hing, C. Lau, and R. Fedkiw, "Creating and simulating skeletal muscle from the visible human data set," *IEEE Trans Visual Comput Graph*, vol. 11, pp. 317–328, 2005.
- [10] S. Blemker and S. Delp, "Three-dimensional representation of complex muscle architectures and geometries," *Ann Biomed Eng*, vol. 33, pp. 661–673, 2005.
- [11] A. Aubel and D. Thalmann, "Interactive modeling of the human musculature," *Comput Animation*, 2001.
- [12] F. Scheepers, R. Parent, W. Carlson, and S. May, "Anatomy-based modeling of the human musculature," in *SIGGRAPH'97*, 1997, pp. 163–172.
- [13] D. Benoit, D. Ramsey, M. Lamontagne, L. Xu, P. Wretenberg, and P. Renstroem, "Effect of skin movement artifact on knee kinematics during gait and cutting motions measured in vivo," *Gait & Posture*, vol. 24, no. 2, pp. 152–164, 2006.
- [14] A. Cappozzo, F. Catani, A. Leardini, M. Benedetti, and U. D. Croce, "Position and orientation in space of bones during movement: experimental artefacts," *Clin Biomech*, vol. 11, no. 2, pp. 90–100, 1996.
- [15] K. Manal, I. McClay, J. Richards, B. Galinat, and S. Stanhope, "Knee moment profiles during walking: errors due to soft tissue movement of the shank and the influence of the reference coordinate system," *Gait & Posture*, vol. 15, pp. 10–17, 2002.
- [16] L. Lucchetti, A. Cappozzo, A. Cappello, and U. D. Croce, "Skin movement artefact assessment and compensation in the estimation of kneejoint kinematics," *J Biomech*, vol. 31, no. 11, pp. 977–984, 1998.
- [17] E. Alexander and T. Andriacchi, "Correcting for deformation in skin-based marker systems," *J Biomech*, vol. 34, pp. 355–361, 2001.
- [18] T. Lu and J. O'Connor, "Bone position estimation from skin marker coordinates using global optimisation with joint constraints," *J Biomech*, vol. 32, pp. 129–134, 1999.
- [19] (2006-2010) 3d anatomical human project website. [Online]. Available: <http://3dah.miralab.unige.ch/>
- [20] (2001-2009) Come swiss national project. [Online]. Available: <http://come.ch/>
- [21] F. Shellock and J. Crues, "Mr procedures: Biologic effects, safety, and patient care," *Radiology*, vol. 232, pp. 635–652, 2004.
- [22] A. Heemskerk, G. Strijkers, A. Vilanova, M. Drost, and K. Nicolay, "Determination of mouse skeletal muscle architecture using three-dimensional diffusion tensor imaging," *Magn Reson Med*, vol. 53, no. 6, pp. 1333–1340, 2005.
- [23] B. Gilles, "Anatomical and kinematical modelling of the musculoskeletal system from mri," Ph.D. dissertation, Université de Genève, 2007.
- [24] B. Gilles, R. Perrin, N. Magnenat-Thalmann, and J.-P. Valle, "Bones motion analysis from dynamic MRI: acquisition and tracking," *Acad Radiol*, vol. 12, pp. 2385–2392, October 2005.
- [25] H. Delingette, "General object reconstruction based on simplex meshes," *Int J Comput Vis*, vol. 32, no. 2, pp. 111–146, 1999.
- [26] E. Grood and W. Suntay, "A joint coordinate system for the clinical description of three-dimensional motions: application to the knee," *J Biomech Eng*, vol. 105, pp. 136–144, 1983.
- [27] G. Wu, S. Siegler, P. Allard, C. Kirtley, A. Leardini, D. Rosenbaum, M. Whittle, D. D'Lima, L. Cristofolini, H. Witte, O. Schmid, and I. Stokes, "ISB recommendation on definitions of joint coordinate system of various joints for the reporting of human joint motion - part I: Ankle, hip and spine," *J Biomech*, vol. 35, no. 4, pp. 543–548, 2002.
- [28] M. Hauth and O. Eitzmuss, "A high performance solver for the animation of deformable objects using advanced numerical methods," in *Eurographics'01*, 2001, pp. 137–151.
- [29] P. Volino and N. Magnenat-Thalmann, "Implicit midpoint integration and adaptive damping for efficient cloth simulation," *Comput Animation Virt World*, vol. 16, no. 3-4, pp. 163–175, 2005.
- [30] B. Gilles, L. Moccozet, and N. Magnenat-Thalmann, "Anatomical modelling of the musculoskeletal system from MRI," in *Med Image Comput Comp Assist Intervention (MICCAI'06)*, 2006, pp. 289–296.
- [31] T. Cootes, A. Hill, C. Taylor, and J. Haslam, "The use of active shape models for locating structures in medical images," in *Int Conf Inform Process Med Imag (IPMI'93)*, 1993, pp. 33–47.
- [32] J. Fripp, S. Crozier, S. Warfield, and S. Ourselin, "Automatic segmentation of the bone and extraction of the bone-cartilage interface from magnetic resonance images of the knee," *Phys Med Biol*, vol. 52, pp. 1617–1631, 2007.
- [33] D. Baraff and A. Witkin, "Large steps in cloth simulation," in *SIGGRAPH'98*, 1998, pp. 43–54.
- [34] M. Teschner, S. Kimmerle, B. Heidelberger, G. Zachmann, L. Raghupathi, A. Fuhrmann, M. Cani, F. Faure, N. Magnenat-Thalmann, W. Strasser, and P. Volino, "Collision detection for deformable objects," *Comput Graph Forum*, vol. 24, no. 1, pp. 61–81, 2005.
- [35] P. Volino and N. Magnenat-Thalmann, "Implementing fast cloth simulation with collision response," in *Comput Graph Int*, 2000, pp. 257–266.
- [36] H. Seo and N. Magnenat-Thalmann, "An automatic modeling of human bodies from sizing parameters," in *ACM SIGGRAPH 2003 Symp on Interact 3D Graph*, April 2003, pp. 19–26.
- [37] A. Leardini, L. Chiari, U. D. Croce, and A. Cappozzo, "Human movement analysis using stereophotogrammetry Part 3. Soft tissue artifact assessment and compensation," *Gait & Posture*, vol. 21, pp. 212–225, 2005.
- [38] C. Lawrence and A. Tits, "A computationally efficient feasible sequential quadratic programming algorithm," *SIAM J Optim*, vol. 11, no. 4, pp. 1092–1118, 2001.
- [39] D. Reynolds, J. Lucas, and K. Klaue, "Retroversion of the acetabulum: A cause of hip pain," *J Bone Joint Surg*, vol. 81-B, no. 2, pp. 281–288, 1999.
- [40] C. W. A. Pfirrmann, B. Mengiardi, C. Dora, F. Kalberer, M. Zanetti, and J. Hodler, "Cam and pincer femoroacetabular impingement: Characteristic mr arthrographic findings in 50 patients," *Radiology*, vol. 240, no. 3, pp. 778–785, 2006.